Article

Switching in Molecular Transport Junctions: Polarization Response

Sina Yeganeh, Michael Galperin, and Mark A. Ratner

J. Am. Chem. Soc., **2007**, 129 (43), 13313-13320• DOI: 10.1021/ja0730967 • Publication Date (Web): 04 October 2007

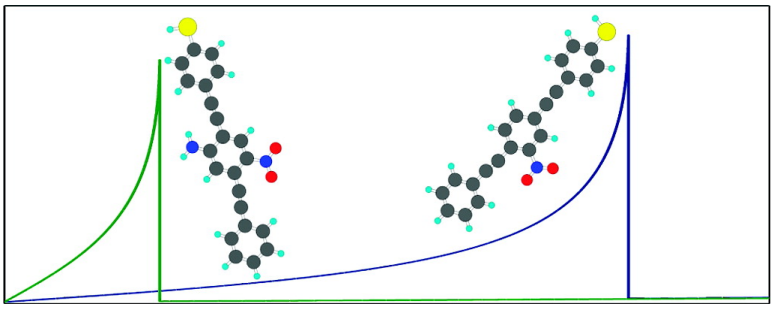

J|A|C|S
ARTICLES
Published on Web 10/04/2007

Switching in Molecular Transport Junctions: Polarization Response

Sina Yeganeh, Michael Galperin, and Mark A. Ratner*

Contribution from the Department of Chemistry, Center for Nanofabrication and Molecular Self Assembly, and Materials Research Science and Engineering Center, Northwestern University, Evanston, Illinois 60208-3113

Received May 2, 2007; E-mail: ratner@northwestern.edu

Abstract: We discuss several proposed explanations for the switching and negative differential resistance (NDR) behavior seen in some molecular junctions. Several theoretical models are discussed, and we present results of electronic structure calculations on a series of substituted oligo(phenylene ethynylene) molecules. It is shown that a previously proposed polaron model is successful in predicting NDR behavior, and the model is elaborated with image charge effects and parameters from electronic structure calculations. This model now incorporates substituent effects and includes the effects of conformational change, charging, and image charge stabilization.

1. Introduction

Since the first discussions of molecular-based alternatives[1−3] to traditional semiconductor electronics, many experiments have investigated the properties of a variety of molecules in junctions. Molecular-based devices can be an important ingredient in extending advances in electronics to smaller scales,[4] and molecules possess additional unique characteristics such as internal degrees of freedom, dynamical stereochemistry, and the potential to form actuators. Recently, there has been a focus on nonstochastic switching in molecular junctions spurred partially by the discovery of a robust negative differential resistance (NDR) characteristic with a peak-to-valley ratio (PVR) of 1030:1 and switching behavior in a self-assembled monolayer (SAM) of 2′-amino-4,4′-di(ethynylphenyl)-5′-nitro-1-benzenethiol.[5−10] Such NDR behavior is the basis for a molecular switch and could provide an important component in a molecular electronics toolkit. Several groups have shown[5−17] that NDR is only observed in oligo(phenylene ethynylene) (OPE) SAM systems with particular molecular substituents (nitro groups), thus suggesting the NDR has a molecular origin and is not due to stochastic switching.[18] NDR has also been observed in single molecule junctions.[19] We note that NDR has been experimentally observed in a number of other molecular systems,[20−24] but we focus our attention on the NDR seen in the series of molecules shown in Figure 1. A brief summary of the experimental results for these systems is presented in Table 1.

Several explanations have been proposed to explain the observed NDR including charging to form the radical anion[25−28] or cation[29] and conformational change[25,30−41] of the molecule.

(1) Aviram, A.; Ratner, M. A. *Chem. Phys. Lett.* **1974**, *29*, 277−283.
(2) Carter, F. L. *J. Vac. Sci. Technol., B* **1983**, *1*, 959−968.
(3) Bloor, D. *Introduction to Molecular Electronics*; Petty, M. C., Bryce, M. R., Bloor, D., Eds.; Oxford Univerity Press: New York, 1995; Chapter 1, pp 1−28.
(4) Joachim, C.; Ratner, M. A. *Proc. Natl. Acad. Sci. U.S.A.* **2005**, *102*, 8801−8808.
(5) Chen, J.; Reed, M. A.; Rawlett, A. M.; Tour, J. M. *Science* **1999**, *286*, 1550−1552.
(6) Chen, J.; Wang, W.; Reed, M. A.; Rawlett, A. M.; Price, D. W.; Tour, J. M. *Appl. Phys. Lett.* **2000**, *77*, 1224−1226.
(7) Chen, J.; Wang, W.; Klemic, J.; Reed, M. A.; Axelrod, B. W.; Kaschak, D. M.; Rawlett, A. M.; Price, D. W.; Dirk, S. M.; Tour, J. M.; Grubisha, D. S.; Bennett, D. W. *Ann. N.Y. Acad. Sci.* **2002**, *960*, 69−99.
(8) Chen, J.; Reed, M. A. *Chem. Phys.* **2002**, *281*, 127−145.
(9) Chen, J.; Su, J.; Wang, W.; Reed, M. A. *Physica E* **2003**, *16*, 17−23.
(10) Chen, J.; Reed, M. A.; Dirk, S. M.; Price, D. W.; Rawlett, A. M.; Tour, J. M.; Grubisha, D. S.; Bennett, D. W. *Advanced Semiconductor and Organic Nano-Techniques*; Morkoc, H., Ed.; Academic Press: New York, 2003; Vol. 3, Chapter 2, pp 43−187.
(11) Fan, F. F.; Yang, J.; Dirk, S.; Price, D.; Kosynkin, D.; Tour, J.; Bard, A. *J. Am. Chem. Soc.* **2001**, *123*, 2454−2455.
(12) Fan, F. F.; Yang, J. P.; Cai, L. T.; Price, D. W.; Dirk, S. M.; Kosynkin, D. V.; Yao, Y. X.; Rawlett, A. M.; Tour, J. M.; Bard, A. J. *J. Am. Chem. Soc.* **2002**, *124*, 5550−5560.
(13) Fan, F. F.; Lai, R. Y.; Cornil, J.; Karzazi, Y.; Bredas, J. L.; Cai, L. T.; Cheng, L.; Yao, Y. X.; Price, D. W.; Dirk, S. M.; Tour, J. M.; Bard, A. J. *J. Am. Chem. Soc.* **2004**, *126*, 2568−2573.
(14) Fan, F. F.; Yao, Y.; Cai, L.; Cheng, L.; Tour, J. M.; Bard, A. J. *J. Am. Chem. Soc.* **2004**, *126*, 4035−4042.
(15) Rawlett, A. M.; Hopson, T. J.; Nagahara, L. A.; Tsui, R. K.; Ramachandran, G. K.; Lindsay, S. M. *Appl. Phys. Lett.* **2002**, *81*, 3043−3045.
(16) Le, J. D.; He, Y.; Hoye, T. R.; Mead, C. C.; Kiehl, R. A. *Appl. Phys. Lett.* **2003**, *83*, 5518−5520.
(17) Kiehl, R. A.; Le, J. D.; Candra, P.; Hoye, R. C.; Hoye, T. R. *Appl. Phys. Lett.* **2006**, *88*, 172102.
(18) Ramachandran, G. K.; Hopson, T. J.; Rawlett, A. M.; Nagahara, L. A.; Primak, A.; Lindsay, S. M. *Science* **2003**, *300*, 1413−1416.
(19) Xiao, X.; Nagahara, L. A.; Rawlett, A. M.; Tao, N. *J. Am. Chem. Soc.* **2005**, *127*, 9235−9240.
(20) Xue, Y.; Datta, S.; Hong, S.; Reifenberger, R.; Henderson, J. I.; Kubiak, C. P. *Phys. Rev. B* **1999**, *59*, R7852−R7855.
(21) Gaudioso, J.; Lauhon, L. J.; Ho, W. *Phys. Rev. Lett.* **2000**, *85*, 1918−1921.
(22) Richter, C. A.; Stewart, D. R.; Ohlberg, D. A.; Williams, R. S. *Appl. Phys. A: Mater. Sci. Process.* **2005**, *80*, 1355−1362.
(23) Tran, E.; Duati, M.; Whitesides, G.; Rampi, M. *Faraday Discuss.* **2006**, *131*, 197−203.
(24) Li, Y. F.; Hatakeyama, R.; Kaneko, T.; Kato, T.; Okada, T. *Appl. Phys. Lett.* **2007**, *90*, 073106.
(25) Seminario, J. M.; Zacarias, A. G.; Tour, J. M. *J. Am. Chem. Soc.* **2000**, *122*, 3015−3020.
(26) Seminario, J. M.; Zacarias, A. G.; Derosa, P. A. *J. Chem. Phys.* **2002**, *116*, 1671−1683.
(27) Simon-Manso, Y.; Gonzalez, C.; Mujica, V.; Aray, Y.; Marquez, M. *Ann. N.Y. Acad. Sci.* **2003**, *1006*, 68−81.
(28) Walczak, K.; Lyshevski, S. E. *Cent. Eur. J. Phys.* **2005**, *3*, 555−563.
(29) Ghosh, A. W.; Zahid, F.; Datta, S.; Birge, R. R. *Chem. Phys.* **2002**, *281*, 225−230.

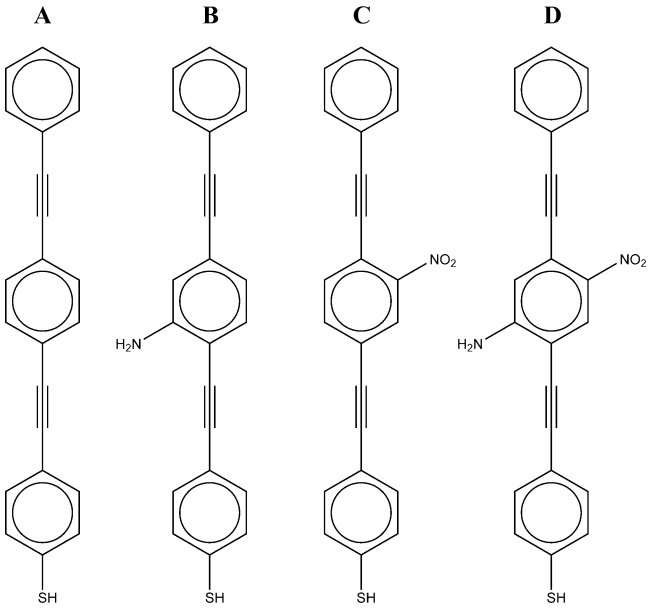

Figure 1. Molecular structures examined in this study.

Table 1. Summary of Experimental Results for Molecules in Figure 1[a]

molecule	technique	NDR	hysteresis
A	SAM	○[5,7−9]	○[7−9]
	SM	○[15,19]	○[19]
B	SAM	○[7−9]	○[7−9]
C	SAM	○[112], ●[6−9,12,113]	●[7−9,112,114]
	SM	○[103−105], ●[15,19,115]	○[103−105], ●[19]
D	SAM	●[5−9,16,17,12,114]	●[7−9,17,114,116]

[a] The symbols ○ and ● refer to the absence and observation (respectively) of NDR or hysteresis. Results are shown for self-assembled monolayers (SAM) as well as single molecule (SM) junctions where available. For single molecule junctions, we include true single molecule arrangements as well as experiments in which the relevant molecule is embedded in an insulating SAM.

Aside from qualitative predictions based on analysis of molecular orbitals and their spatial characteristics, some of these works have made use of the nonequilibrium Green's function (NEGF) formalism[42−48] combined with an electronic structure method, usually density functional theory (DFT) or extended Hückel theory (EHT), for computing the current−voltage behavior. Although the NEGF method is not the only theoretical approach for calculating molecular conductance,[49−51] it provides a proper treatment of nonequilibrium systems. However, the remarkably sharp NDR characteristic has not been reproduced (with a few exceptions),[52] and these models are also unable to explain bistability although some attempts have been made to reproduce the observed hysteresis.[53] Since the calculations are treating the electronic states of the system accurately (except for possible issues with the use of DFT in nonequilibrium systems)[54−60] this suggests that some important physics is missing in the mechanisms proposed thus far. As NDR behavior has been observed so far only in the nitro-substituted compounds,[5−17] the necessity of a redox center suggests polaron formation as the basis for NDR in these systems.[61] Several authors have applied a polaron model to quantum dots and molecular junctions,[62−69] and in particular, using a polaron Hamiltonian within the static limit of the Born−Oppenheimer (BO) approximation, Galperin et al.[61,70] were able to qualitatively reproduce the observed current−voltage characteristics. Herein we discuss several model treatments and analyze their ability to predict both NDR and hysteresis in molecular junctions. Introducing a modified polaron model, we explain the observed NDR behavior and functionality dependence. Finally, we discuss failings of the model and suggest further experiments in switching systems.

2. Models for Explaining NDR and Switching

2.1. Charging. Charging was recognized as a possible mechanism for NDR in the first experimental report[5] which proposed a double reduction process: increasing voltage initially causes a reduction which supplies a charge carrier until a second reduction occurs, resulting in singlet dianion and drop in current. Computational analyses have focused on the spatial profile of the molecular orbitals for the neutral, anion, and dianion species,[25,26,71] and qualitative predictions of the molecular conductance properties have been made. Predictions of transport

(30) Seminario, J. M.; Derosa, P. A.; Bastos, J. L. *J. Am. Chem. Soc.* **2002**, *124*, 10266−10267.
(31) Majumder, C.; Briere, T.; Mizuseki, H.; Kawazoe, Y. *J. Phys. Chem. A* **2002**, *106*, 7911−7914.
(32) Stokbro, K.; Taylor, J.; Brandbyge, M.; Ordejó, P. *Ann. N.Y. Acad. Sci.* **2003**, *1006*, 212−225.
(33) Taylor, J.; Brandbyge, M.; Stokbro, K. *Phys. Rev. B* **2003**, *68*, 121101.
(34) Cornil, J.; Karzazi, Y.; Bredas, J. L. *J. Am. Chem. Soc.* **2002**, *124*, 3516−3517.
(35) Karzazi, Y.; Cornil, J.; Bredas, J. L. *Nanotechnology* **2003**, *14*, 165−171.
(36) Ricca, A.; Bauschlicher, C. W. *J. Phys. Chem. B* **2005**, *109*, 9059−9065.
(37) Bauschlicher, C. W.; Ricca, A. *Phys. Rev. B* **2005**, *71*, 205406.
(38) Yin, X.; Li, Y. W.; Zhang, Y.; Li, P.; Zhao, J. W. *Chem. Phys. Lett.* **2006**, *422*, 111−116.
(39) Yin, X.; Liu, H.; Zhao, J. W. *J. Chem. Phys.* **2006**, *125*, 094711.
(40) Lu, J. Q.; Wu, J.; Chen, H.; Duan, W. H.; Gu, B. L.; Kawazoe, Y. *Phys. Lett. A* **2004**, *323*, 154−158.
(41) Amadei, A.; D'Abramo, M.; Nola, A. D.; Arcadi, A.; Cerichelli, G.; Aschi, M. *Chem. Phys. Lett.* **2007**, *434*, 194−199.
(42) Kadanoff, L. P.; Baym, G. *Quantum Statistical Mechanics;* W. A. Benjamin, Inc.: New York, 1962.
(43) Keldysh, L. *Sov. Phys. JETP* **1965**, *20*, 1018−1026.
(44) Danielewicz, P. *Ann. Phys.* **1984**, *152*, 239−304.
(45) Rammer, J.; Smith, H. *Rev. Mod. Phys.* **1986**, *58*, 323−359.
(46) Haug, H.; Jauho, A.-P. *Quantum Kinetics in Transport and Optics of Semiconductors;* Springer: Berlin, 1996.
(47) Xue, Y. Q.; Datta, S.; Ratner, M. A. *Chem. Phys.* **2002**, *281*, 151−170.
(48) Datta, S. *Quantum Transport: Atom to Transistor;* Cambridge University Press: Cambridge 2005.
(49) Di Ventra, M.; Pantelides, S. T.; Lang, N. D. *Phys. Rev. Lett.* **2000**, *84*, 979−982.
(50) Nitzan, A. *Ann. Rev. Phys. Chem.* **2001**, *52*, 681−750.
(51) Nitzan, A.; Ratner, M. A. *Science* **2003**, *300*, 1384−1389.
(52) Gonzalez, C.; Simon-Manso, Y.; Batteas, J.; Marquez, M.; Ratner, M. A.; Mujica, V. *J. Phys. Chem. B* **2004**, *108*, 18414−18420.
(53) Seminario, J. M.; Cordova, L. E.; Derosa, P. A. *Proc. IEEE* **2003**, *91*, 1958−1975.
(54) Reimers, J. R.; Cai, Z. L.; Bilic, A.; Hush, N. S. *Ann. N.Y. Acad. Sci.* **2003**, *1006*, 235−251.
(55) Krstic, P. S.; Dean, D. J.; Zhang, X. G.; Keffer, D.; Leng, Y. S.; Cummings, P. T.; Wells, J. C. *Comput. Mat. Sci.* **2003**, *28*, 321−341.
(56) Toher, C.; Filippetti, A.; Sanvito, S.; Burke, K. *Phys. Rev. Lett.* **2005**, *95*, 146402.
(57) Evers, F.; Weigend, F.; Koentopp, M. *Phys. Rev. B* **2004**, *69*, 235411.
(58) Koentopp, M.; Burke, K.; Evers, F. *Phys. Rev. B* **2006**, *73*, 121403.
(59) Baer, R.; Livshits, E.; Neuhauser, D. *Chem. Phys.* **2006**, *329*, 266−275.
(60) Emberly, E. G.; Kirczenow, G. *Phys. Rev. B* **2001**, *6412*, 125318.
(61) Galperin, M.; Ratner, M. A.; Nitzan, A. *Nano Lett.* **2005**, *5*, 125−130.
(62) Alexandrov, A. S.; Bratkovsky, A. M.; Williams, R. S. *Phys. Rev. B* **2003**, *67*, 075301.
(63) Alexandrov, A. S.; Bratkovsky, A. M. *Phys. Rev. B* **2003**, *67*, 235312.
(64) Mitra, A.; Aleiner, I.; Millis, A. J. *Phys. Rev. B* **2004**, *69*, 245302.
(65) Mitra, A.; Aleiner, I.; Millis, A. J. *Phys. Rev. Lett.* **2005**, *94*, 076404.
(66) Zazunov, A.; Feinberg, D.; Martin, T. *Phys. Rev. B* **2006**, *73*, 115405.
(67) Mozyrsky, D.; Hastings, M. B.; Martin, I. *Phys. Rev. B* **2006**, *73*, 035104.
(68) Gogolin, A. O.; Komnik, A. Multistable transport regimes and conformational changes in molecular quantum dots. 2002, cond-mat/0207513..7513G. arXiv e-print. http://adsabs.harvard.edu/abs/2002cond.mat..
(69) Ness, H.; Shevlin, S. A.; Fisher, A. J. *Phys. Rev. B* **2001**, *63*, 125422.
(70) Galperin, M.; Ratner, M. A.; Nitzan, A. *J. Phys.: Condens. Matter* **2007**, *19*, 103201.
(71) Seminario, J. M.; Zacarias, A. G.; Derosa, P. A. *J. Phys. Chem. A* **2001**, *105*, 791−795.

properties based on ground-state electronic structure properties, however, are not expected to reflect accurately the junction under applied voltage,[49,72] and the degree of localization in frontier orbitals is strongly dependent on the level of theory used.[73] In one work,[26] a DFT/equilibrium Green's function (EGF) approach yielded a slight NDR for the nitroamine substituted compound (**D** in Figure 1); however, this calculation was not done self-consistently in the presence of bias, as the isolated molecular orbitals were inserted into the EGF expressions. Additionally, the authors argue that on the basis of experimental data[5,6] the anion molecular orbitals can be used at some appropriate switching voltage, thus yielding a larger NDR drop. However, in a molecular junction coupled to semi-infinite electrodes, the charge state of the molecule is ill-defined, and the mean electron occupation must be calculated self-consistently. Proper self-consistent calculations with a DFT/NEGF approach[32,33] have shown that the electron population changes by 0.05 at most, suggesting that substantial charging without additional stabilization (such as polaron formation through the electron−phonon interaction) does not occur.

Other work[39] using self-consistent DFT/NEGF did not observe any NDR effect but found mild rectification. Similarly, using a simple EHT/NEGF model, Walczak and Lyshevski[28] found mild rectification but no NDR. Interestingly, although most research has focused on charging in the nitroamine molecule via reduction, Ghosh et al.[29] argue that the transport involves oxidation through the HOMO level. With the exception of ref 26, these approaches have been unsuccessful in reproducing the observed NDR. A related explanation, charge density rearrangement at the NDR threshold voltage,[27,52] has also been used to explain the switching with moderate success, although the use of equilibrium Green's functions is questionable at the higher voltage regime in which NDR is seen, as noted by the authors. A similar argument, using a donor−acceptor model for the nitroamine molecule, also yielded a large NDR.[74] In addition, the charging model cannot explain the hysteresis observed at higher temperatures,[9] relevant for molecular memory devices.

2.2. Conformational Change. A second proposed explanation for the switching behavior involves conformational change induced by voltage or electric field. Early computational work examined the degree of localization of the HOMO/LUMO levels as a function of the rotation of the central ring[30,34,35,40] as well as side rings[31] in isolated functionalized OPE molecules. In particular, Lu et al.[40] found a large decrease in the conductance as the central ring of monothiol nitroamine molecule was rotated from planarity; however, it is important to note that only the zero-bias conductance was calculated, and the voltage dependence of the twisting was not shown. Yin *et. al*[38] have included the effect of geometry relaxation in response to an electric field and found no significant twisting at high electric field; the current−voltage relationship showed no NDR or significant change between the frozen and relaxed geometries.

Additionally, the effect of rotation in various charge states of the molecule, a combination of the charging and conformational models, has been examined.[25] In general, these studies showed significant localization in the LUMO of the rotated conformer; assuming conduction through the LUMO, the sudden decrease in current was thus ascribed to the loss of delocalization upon rotation of the rings. These works have neglected intermolecular interactions, relevant in conformational effects in monolayers. Thus, recent work has examined the rotational barriers of the molecules in self-assembled monolayers;[37,36] for tilted monolayers, a local potential minimum at 90° twist of the central ring was predicted. Similarly, Taylor et al.[33] found that monolayers of the nitroamine molecule are stabilized at 60° and 120° rotation of the central ring. They also calculated the total energies of the monolayers at 0° and 60° and found an expected switch near the observed NDR voltage between the stable conformations. Although a substantial NDR is observed between the current in the planar and twisted conformations at this voltage, hysteresis cannot be explained by these conformational change models.

2.3. Polaron Formation. We briefly introduce the polaron theory as it relates to NDR and hysteresis phenomena. Physically, the polaron model consists of charging followed by conformational change: an electron is injected onto the molecule, and the timescales are such that the molecule can geometrically relax before tunneling to the opposite electrode occurs.[75] Indeed, a recent calculation on unsubstituted and nitroamine OPE has pointed out that charge transfer in OPE is highly dependent on molecular conformation.[41] We are not the first to point out the importance of both these models; Emberly and Kirczenow[60] have previously discussed both charging and conformational change to treat transport nonlinearities. We suggest that the underlying phenomenon should be treated with a polaron model to explain both the NDR as well as hysteresis bistability.[61] Other authors have used a similar model to predict both NDR[66] and hysteresis.[67,68] While trying to describe resonant transport with vibronic coupling, Benesch et al. noted a significant NDR effect as a result of energy-dependent molecule−lead coupling (absent in the wide-band limit commonly taken, as here), but this type of NDR disappeared when vibrational effects were included.[76] Treatments of semiconductor−molecule junctions have also noted the appearance of NDR as a result of the semiconductor band-edge.[77,78] We use the previous polaron work[61] and extend it to include explicitly the energy change upon change of charge state as well as additional stabilization induced by image charge effects with the metal electrodes. This allows for quantitative distinctions to be made between the substituted OPE systems.

3. Polaron Model

We follow the work of Galperin et al.,[61] but allow for multiple molecular vibrational modes. The molecular bridge is represented by a single electronic state of energy ϵ_0 coupled to the $3N - 6$ vibrational modes, each with frequency ω_n and vibronic coupling M_n, as well as to the left and right contacts (energy

(72) Di Ventra, M.; Kim, S. G.; Pantelides, S. T.; Lang, N. D. *Phys. Rev. Lett.* **2001**, *86*, 288−291.
(73) Bauschlicher, C. W.; Lawson, J. W. *Phys. Rev. B* **2007**, *75*, 115406.
(74) Lakshmi, S.; Pati, S. K. *Phys. Rev. B* **2005**, *72*, 193410.
(75) Karzazi, Y.; Cornil, J.; Bredas, J. *J. Am. Chem. Soc.* **2001**, *123*, 10076−10084.
(76) Benesch, C.; Cizek, M.; Thoss, M.; Domcke, W. *Chem. Phys. Lett.* **2006**, *430*, 355−360.
(77) Rakshit, T.; Liang, G. C.; Ghosh, A. W.; Datta, S. *Nano Lett.* **2004**, *4*, 1803−1807.
(78) Rakshit, T.; Liang, G.-C.; Ghosh, A. W.; Hersam, M. C.; Datta, S. *Phys. Rev. B.* **2005**, *72*, 125305.

levels given by $\epsilon_{k\in L}$ and $\epsilon_{k\in R}$, respectively) on each side with coupling V_k. The Hamiltonian that follows is given by

$$\hat{H} = \epsilon_0 \hat{c}_0^\dagger \hat{c}_0 + \sum_{n=1}^{3N-6} \omega_n \hat{a}_n^\dagger \hat{a}_n + \sum_{k\in\{L,R\}} \epsilon_k \hat{c}_k^\dagger \hat{c}_k + \sum_{k\in\{L,R\}} (V_k \hat{c}_k^\dagger \hat{c}_0 + h.c.) + \sum_{n=1}^{3N-6} M_n (\hat{a}_n^\dagger + \hat{a}_n) \hat{c}_0^\dagger \hat{c}_0 \quad (1)$$

In the above expression, $\hat{c}_0^\dagger/\hat{c}_0$ is the electron creation/annihilation operator for the single electronic state in the molecular region, $\hat{a}_n^\dagger/\hat{a}_n$ is the molecular phonon[79] creation/annihilation operator, and $\hat{c}_k^\dagger/\hat{c}_k$ is the electron creation/annihilation operator for the contacts. We have chosen reduced units such that $\hbar = 1$ and $m_e = 1$.

Within the static limit of the BO approximation, the phonon Hamiltonian can be written in terms of the average electronic population, $n_0 = \langle c_0^\dagger \hat{c}_0 \rangle$:

$$\hat{H}_{ph} = \sum_{n=1}^{3N-6} \omega_n \hat{a}_n^\dagger \hat{a}_n + \sum_{n=1}^{3N-6} M_n (\hat{a}_n^\dagger + \hat{a}_n) n_0 \quad (2)$$

and a separable equation of motion can be written for the dynamics of each phonon mode (in the absence of intramode coupling):

$$-\frac{1}{2\omega_n}\left(\frac{d^2}{dt^2} + {\omega_n}^2\right)(\hat{a}_n^\dagger + \hat{a}_n)(t) = M_n n_0(t) \quad (3)$$

The retarded Green function of the nth primary phonon, $D_n^r(t)$, is given by

$$-\frac{1}{2\omega_n}\left(\frac{d^2}{dt^2} + {\omega_n}^2\right) D_n^r(t-t') = \delta(t-t') \quad (4)$$

and in terms of the retarded phonon Green function, we can write

$$(\hat{a}_n^\dagger + \hat{a}_n)(t) = (\hat{a}_n^\dagger + \hat{a}_n)_0(t) + \int_{-\infty}^{\infty} dt'\, D_n^r(t-t') M_n n_0(t') \quad (5)$$

where $(\hat{a}_n^\dagger + \hat{a}_n)_0(t)$ is the solution for the primary phonon dynamics in the absence of any couplings. In steady-state,

$$\langle (\hat{a}_n^\dagger + \hat{a}_n) \rangle = M_n n_0 D_n^r(\omega = 0) = -\frac{2M_n}{\omega_n} n_0 \quad (6)$$

and substituting this expression into the original Hamiltonian (eq 1) results in an effective electronic Hamiltonian within the BO approximation:

$$\hat{H}_{el} = \overline{\epsilon_0}(n_0) \hat{c}_0^\dagger \hat{c}_0 + \sum_{k\in\{L,R\}} \epsilon_k \hat{c}_k^\dagger \hat{c}_k + \sum_{k\in\{L,R\}} (V_k \hat{c}_k^\dagger \hat{c}_0 + h.c.) \quad (7)$$

where the bridge energy has been shifted by the polaron reorganization energy, ϵ_{reorg}:

$$\overline{\epsilon_0}(n_0) = \epsilon_0 - 2n_0\epsilon_{reorg} \quad (8)$$

$$\epsilon_{reorg} = \sum_{n=1}^{3N-6} \frac{{M_n}^2}{\omega_n} = \lambda \quad (9)$$

These renormalized energies are then used to construct the Green's functions for the device region, $G^r, G^a, G^<$, and self-energy, $\Sigma^<$, in the wide-band limit for the molecule−lead coupling:

$$G^r(E) = [E - \overline{\epsilon_0}(n_0) + i(\Gamma_L + \Gamma_R)/2]^{-1},\ G^a(E) = [G^r(E)]^* \quad (10)$$

$$G^<(E) = G^r(E)\Sigma^<(E)G^a(E) \quad (11)$$

$$\Sigma^<(E) = \Sigma_L^<(E) + \Sigma_R^<(E) = i(f_L(E)\Gamma_L + f_R(E)\Gamma_R) \quad (12)$$

and n_0 can then be written:

$$n_0 = -i\int_{-\infty}^{\infty} \frac{dE}{2\pi} G^<(E) = \int_{-\infty}^{\infty} \frac{dE}{2\pi} \frac{f_L(E)\Gamma_L + f_R(E)\Gamma_R}{[E - \overline{\epsilon_0}(n_0)]^2 + [(\Gamma_L + \Gamma_R)/2]^2} \quad (13)$$

In the above equations, $\Gamma_{L,R}$ are couplings to the left and right contacts, and $f_{L,R}$ are Fermi functions in the left and right contacts. Equations 8 and 13 are solved iteratively for the roots of n_0 until self-consistency is reached. The final Green's functions are constructed with the converged renormalized energy, $\overline{\epsilon_0}(n_0)$, and the current is calculated in the usual fashion in the Landauer regime:[80]

$$I = \frac{2e}{\hbar} \int_{-\infty}^{\infty} \frac{dE}{2\pi} (\Gamma_L G^r(E) \Gamma_R G^a(E))(f_L(E) - f_R(E)) \quad (14)$$

Thorough reviews of the NEGF procedure are available for a complete description.[44−46,48,81−83]

It is useful to examine the results of a sample calculation with this model. In Figure 2, we show current−voltage characteristics with parameters that were previously found to produce NDR features.[61] By shifting the single-state energy, ϵ_0, both a reduction and an oxidation mechanism can be used to produce identical NDR responses, as diagrammed in Figure 3. Although not shown here, the model also predicts hysteresis, as discussed in the earlier work,[61] where bistability results from multiple stable solutions for n_0.

However, this simple model is missing an important component of stabilization achieved upon charging. Our single-state Hamiltonian thus far neglects the vertical energy difference between N- and $(N \pm 1)$-electron states, negligible in solid-state but significant in the single molecule system here. Thus we are neglecting V_{EA}, the vertical electron affinity, (see Figure 4) in the effective reorganization energy, which should include the

(79) We use the term phonon for any vibrational normal coordinate.

(80) Meir, Y.; Wingreen, N. S. *Phys. Rev. Lett.* **1992**, *68*, 2512−2515.
(81) Datta, S. *Electronic Transport in Mesoscopic Systems;* Cambridge University Press: Cambridge, U.K., 1995.
(82) Datta, S. *Superlattices Microstruct.* **2000**, *28*, 253−278.
(83) Bruus, H.; Flensberg, K. *Many-body Quantum Theory in Condensed Matter Physics: An Introduction;* Oxford University Press: Oxford, U.K., 2004.

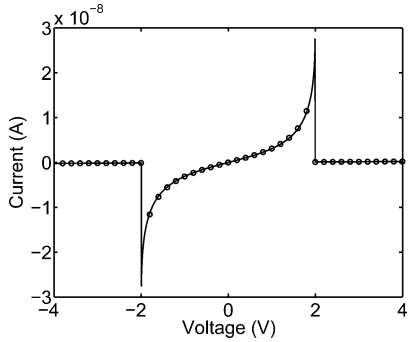

Figure 2. Example of NDR behavior resulting from oxidation (−), beginning in the filled level situation with a sharp drop in current after loss of electron ($\bar{\epsilon_0}$ moves above both electrode's Fermi energies), and reduction (○), beginning with an empty level with a sharp drop in current following occupation and polaron shift ($\bar{\epsilon_0}$ drops below both both Fermi energies). Parameters are from Figure 5 of ref 61, $\Gamma_L = \Gamma_R = 0.01$ eV, $T = 4$ K, and $\epsilon_{reorg} = 5$ eV. For oxidation, we take $\epsilon_0 = 8.75$ eV, and for reduction, $\epsilon_0 = 1.25$ eV. Note that the large value of ϵ_{reorg} is not necessary for NDR, as seen in Figures 5 and 7.

total stabilization energy achieved upon charging. Additionally, image charge stabilization is expected to be significant in these systems[84−86] and should be considered in a similar way. In the static limit, we can proceed by replacing ϵ_{reorg} with $\tilde{\epsilon}_{reorg}$, which includes contributions from the vertical electron affinity and image charge stabilization from the metal electrodes:

$$\tilde{\epsilon}_{reorg} = \lambda + V_{EA} + \epsilon_{image} = \Delta + \epsilon_{image} \tag{15}$$

where Δ is the adiabatic exoergicity of the reaction and ϵ_{image} is the image charge stabilization energy.[87]

Further clarification of ϵ_0, the single state energy, is also necessary. Since we are representing the entire complexity of our molecular bridge with a single state, important considerations such as the response of the molecule's electronic levels to the applied bias are absent. Additionally, the physical interpretation of ϵ_0 in a real molecular system needs to be examined carefully. We argue that ϵ_0 is the energy required to place a charge on the extended molecule system from the infinite gold electrode. This point needs to be further examined as the definition of the extended molecular region is uncertain in the strong molecule−lead coupling case. For charging and polaron formation to occur, however, weak coupling should be the case, the relevant parameters are the molecular electron affinity and the electrode work function, and the single state energy can be associated with the tunneling barrier that the electron experiences without residing on the molecule long enough to experience stabilization:

$$\epsilon_0 = E_{prod} - E_{reac}$$
$$= (E_{anion} + E_{Au^+}) - (E_{neutral} + E_{Au}) = \phi_{Au}^{SAM} - V_{EA} \tag{16}$$

where ϕ_{Au}^{SAM} is the gold work function in the presence of the OPE SAM, included here since we take the Fermi energies of the electrodes to be zero in eq 14.

4. Computational Details

All electronic structure properties were computed with Q-Chem 3.0[88] with DFT and the hybrid exchange-correlation functional B3PW91,[89] which consists of Becke's three-parameter exchange functional[90,91] and the Perdew−Wang 91 correlation functional.[92] The 6-31G** basis set was used. The molecules examined are shown in Figure 1. In our calculations, we have neglected the presence of gold atoms at the molecule−lead interface. The effect of the gold leads on molecular properties in these systems has been discussed by several authors,[71,75,93−96] and some error is introduced by the neglect of the contacts. However, the alternative, electronic structure calculations with a large number of gold atoms, may lead to an artificial accumulation of charge on the contact atoms because of the absence of some of the charge stabilization terms. For each molecule, geometry optimizations were performed for the neutral (singlet, restricted) and singly charged anion (doublet, unrestricted) species. Single-point calculations were carried out to obtain the adiabatic reorganization energies as shown in Figure 4. The image charge stabilization was estimated (see below), and the obtained values are shown in Table 2. The value of ϕ_{Au} was obtained from photoemission experiments[97] of the unsubstituted OPE (**A** in Figure 1) on gold, $\phi_{Au} = 4.2$ eV.

We have also made use of a EHT/NEGF program (Huckel $I-V$ 3.0)[98] to try to explain NDR effects. Huckel $I-V$ 3.0 extends previous implementations[99,100] of an EHT/NEGF code to include electrostatic effects from image charges and the bias potential in the self-consistent potential. Thus, charging and screening are both included in a natural way, and the true potential profile is used. Although a semiempirical electronic structure method is employed, a good description of junction transport can be obtained without invoking DFT and the issues mentioned above.[34,54−60] However, the EHT/NEGF method did not reproduce NDR in any of the molecular systems, and the current had only a mild dependence on the geometry used (neutral or anion) in the calculations. A proper calculation would involve optimizing the geometry at each voltage point as both the charge on the molecule varies and the electrostatic field increases. In the EHT/NEGF calculations, the charge that resides on the molecule remains small (typically around .1e) as there is no charge stabilization from geometry relaxation in the model.

(84) Kubatkin, S.; Danilov, A.; Hjort, M.; Cornil, J.; Bredas, J. L.; Stuhr-Hansen, N.; Hedegard, P.; Bjornholm, T. *Nature* **2003**, *425*, 698−701.
(85) Kubatkin, S.; Danilov, A.; Hjort, M.; Cornil, J.; Bredas, J. L.; Stuhr-Hansen, N.; Hedegard, P.; Bjornholm, T. *Curr. Appl. Phys.* **2004**, *4*, 554−558.
(86) Neaton, J. B.; Hybertsen, M. S.; Louie, S. G. *Phys. Rev. Lett.* **2006**, *97*, 216405.
(87) In keeping with electron transfer literature, we define $\Delta = -\Delta G$, where ΔG is the free energy change. We likewise take ϵ_{image} as the energy released upon image charge stabilization in eq 12.
(88) Shao, Y.; et al. *Phys. Chem. Chem. Phys.* **2006**, *8*, 3172−3191.
(89) For, a discussion of the accuracy of DFT in calculations of the innersphere reorganization energies, see Sancho-Garcia, J. C. *Chem. Phys.* **2007**, *331*, 321−331.
(90) Becke, A. D. *Phys. Rev. A* **1988**, *38*, 3098−3100.
(91) Becke, A. D. *J. Chem. Phys.* **1993**, *98*, 5648−5652.
(92) Perdew, J. P.; Wang, Y. *Phys. Rev. B* **1992**, *45*, 13244−13249.
(93) Seminario, J. M.; De la Cruz, C. E.; Derosa, P. A. *J. Am. Chem. Soc.* **2001**, *123*, 5616−5617.
(94) Larsson, J. A.; Nolan, M.; Greer, J. C. *J. Phys. Chem. B* **2002**, *106*, 5931−5937.
(95) Majumder, C.; Briere, T.; Mizuseki, H.; Kawazoe, Y. *J. Chem. Phys.* **2002**, *117*, 7669−7675.
(96) Ricca, A.; Bauschlicher, C. W. *Chem. Phys. Lett.* **2003**, *372*, 873−877.
(97) Zangmeister, C. D.; Robey, S. W.; van Zee, R. D.; Yao, Y.; Tour, J. M. *J. Phys. Chem. B* **2004**, *108*, 16187−16193.
(98) Zahid, F.; Paulsson, M.; Polizzi, E.; Ghosh, A. W.; Siddiqui, L.; Datta, S. *J. Chem. Phys.* **2005**, *123*, 064707.
(99) Tian, W.; Datta, S.; Hong, S.; Reifenberger, R.; Henderson, J. I.; Kubiak, C. P. *J. Chem. Phys.* **1998**, *109*, 2874−2882.
(100) Zahid, F.; Paulsson, M.; Datta, S. *Advanced Semiconductor and Organic Nano-Techniques*; Morkoc, H., Ed.; Academic Press: New York, 2003; Vol. 3, Chapter 1, pp 1−41.

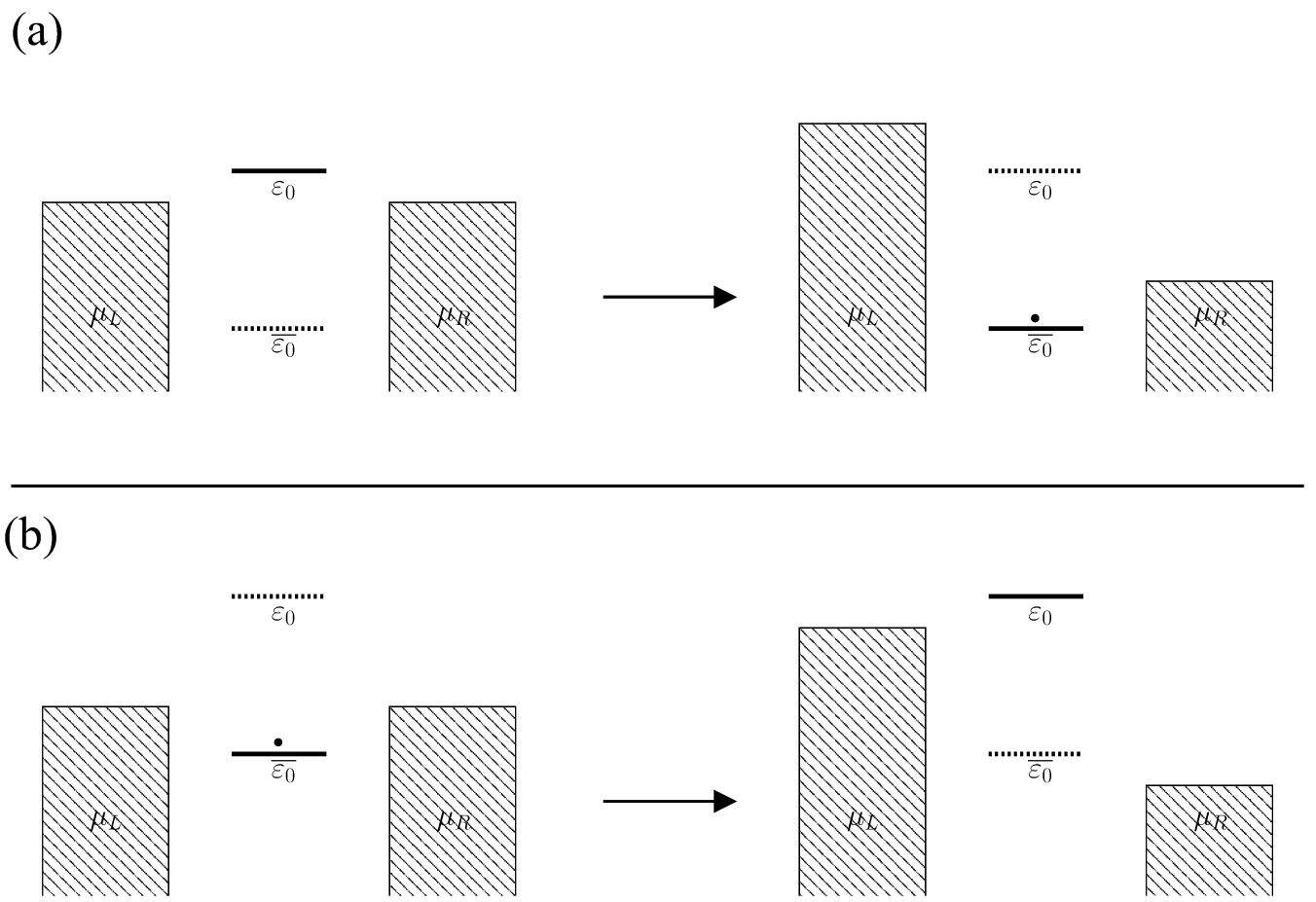

Figure 3. Level diagram for (a) reduction and (b) oxidation with parameters from Figure 2. NDR will be observed when (a) for reduction, the molecule is charged, and $\overline{\epsilon_0}$ drops below both electrodes' Fermi levels ($\epsilon_{reorg} = 5$ eV, $\epsilon_0 = 8.75$ eV). (b) For oxidation, the molecule is initially charged, and ϵ_0 remains above both electrodes' Fermi levels once the charge leaves the molecule ($\epsilon_{reorg} = 5$ eV, $\epsilon_0 = 1.25$ eV).

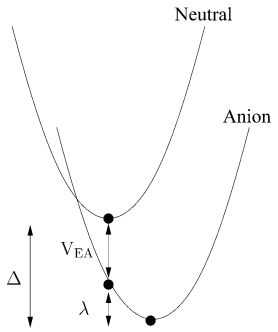

Figure 4. Harmonic model potentials for defining parameters of the polaron model. Δ is the exoergicity of the reaction, V_{EA} is the vertical electron affinity, and λ is the stabilization energy achieved by geometric relaxation to the anion equilibrium structure.

Table 2. Data from Electronic Structure Calculations[a]

molecule	λ	V_{EA}	Δ	ϵ_{image}	$\tilde{\epsilon}_{reorg}$	ϵ_0
A	0.21	0.70	0.91	0.42	1.3	3.5
B	0.24	0.59	0.83	0.42	1.3	3.6
C	0.11	1.33	1.44	0.37	1.8	2.9
D	0.20	1.06	1.26	0.40	1.7	3.1

[a] All values are in eV. ϵ_{image} is calculated from eq 17, and $\tilde{\epsilon}_{reorg}$ is defined by eq 15.[87] Referring to Figure 4, note that the values obtained for λ and V_{EA} indicate that all these systems fall into the marcus inverted regime.

To make our calculations more quantitative, we also include a rough estimate of the image charging energy. Ideally, we would make use of an approach similar to Huckel $I-V$ 3.0 and extract the image charge stabilization by running calculations both with and without the image potential;[98] however, as discussed, only a small amount of charge resides on the molecule in the elastic calculation, and so an estimate of the image charge stabilization is not possible by this method. Alternatively, calculations could be carried out for the neutral and singly charged molecule with gold clusters, so that the image charge stabilization would naturally arise in the anion energetics. However, including a sufficient number of gold atoms is difficult, and additionally without the self-consistent polaron treatment the charge may not localize on the molecular portion of the system. We instead assume an extra electron has been transferred to the isolated molecule and calculate the image charge stabilization in the presence of perfect conductors representing the two gold electrodes. A set of point charges was constructed from the difference in Mulliken populations of the isolated molecule in its neutral and anion states, and the molecule was then displaced from the gold electrodes (assuming a S−Au distance of 2.5 Å on the thiol side and H−Au distance

(101) Note that in the geometry of two parallel metal plates representing contacts, the image charge energy should be renormalized because of higher order image charges in opposite electrodes. See: Arsenin, V. Ya. *Basic Equations and Special Functions of Mathematical Physics;* Iliffe Books: London, 1968. Also see: Galperin, M.; Toledo, S.; Nitzan, A. *J. Chem. Phys.* **2002**, *117*, 10817−10826. Including this renormalization decreases the magnitude of the image charge, but for the rough estimate required here we use the simpler eq 12.

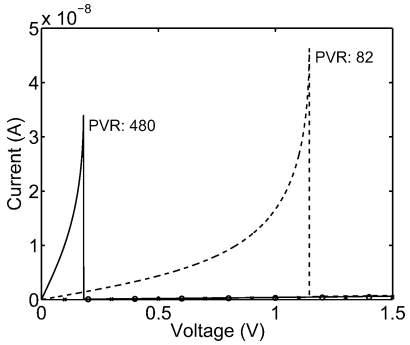

Figure 5. Current−voltage characteristics for the molecules in Figure 1: **A** (○), **B** (x), **C** (---), and **D** (—). The values for ϵ_0 and $\tilde{\epsilon}_{\text{reorg}}$ were taken from Table 2, and the following parameters were used: $\Gamma_L = \Gamma_R = 0.01$ eV and $T = 60$ K. Peak-to-valley ratios (PVR) are shown for the two systems that exhibit NDR. Although negative voltage is not shown, $I(\Phi) = -I(-\Phi)$, where Φ is the applied bias.

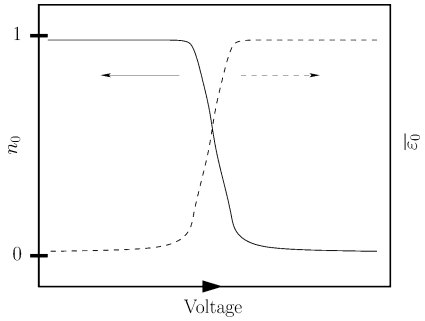

Figure 6. Schematic of the energetic changes in a system exhibiting NDR (such as **C** and **D**). The population n_0 (—) and renormalized energy $\overline{\epsilon_0}$ (---) are shown. The situation for **C** and **D** is shown, where at low voltage, the level is occupied (as in the mechanism diagrammed in Figure 3b), and as voltage is increased, the occupied level approaches resonance with the right electrode chemical potential ($\mu_R \approx \epsilon_0 - 2\tilde{\epsilon}_{\text{reorg}}$). At this point, the level becomes unoccupied and NDR is seen. For **A** and **B**, the system at zero bias begins in the unoccupied state, and the energetics are such that saturation (half-filled level) is reached before NDR can be seen.

of 3 Å on the other).[101] The image charge energy is estimated from the sum of the images,[102]

$$\epsilon_{\text{image}} = -\sum_{\alpha\in\{L,R\}}\sum_{i,j}\frac{1}{4\pi\epsilon_s}\frac{q_i q_j}{4r_{ij}^{\alpha}} \qquad (17)$$

where ϵ_s is the static permittivity (which we take to be $2\epsilon_0$ for the organic SAM), q_i is the Mulliken charge while q_j is the image charge corresponding to Mulliken charge j (with opposite sign). r_{ij}^{α} is the distance between charge i and the point on the electrode surface closest to image charge j. The minus sign is taken in keeping with the sign convention adopted earlier.[87]

5. Results and Discussion

The result of the self-consistent calculations for the current−voltage characteristics of our model systems is shown in Figures 5 and 6. NDR is only seen in the nitro-substituted compounds **C** and **D**; for **A** and **B**, the systems remain in a low-current state until resonance (ϵ_0 between both electrode Fermi levels) is attained at higher voltages. The NDR peaks in experiment varied in position from sample to sample,[8] and so a quantitative comparison of the NDR critical voltage is not possible. Our results suggest that although the basis for NDR is present in many molecular junction systems, there is a narrow parameter range in which a sharp NDR effect will be observed; for example, if the image charge contribution to $\tilde{\epsilon}_{\text{reorg}}$ is neglected, neither **C** nor **D** is found to exhibit NDR. The nitro-substituted molecules show NDR because of the combination of smaller charging energy and larger anion stability. The calculated peak-to-valley ratio at 60 K for **C**, the nitro OPE, is 82:1, while for **D**, nitroamine OPE, it is 480:1. This trend is also seen in experiment, where the nitroamine has a much larger NDR response, although for **C** the NDR was only seen at higher temperatures (190 K). We also note that our NDR results for **C** and **D** begin in the occupied state, and NDR occurs when the charge leaves the molecular region as in Figure 3b. This requires that the system initially be in the charged state, perhaps as a result of an earlier applied voltage. Although not shown, our choice of symmetric molecule−lead couplings ($\Gamma_L = \Gamma_R$) will necessarily lead to current−voltage curves with odd symmetry ($I(\Phi) = -I(-\Phi)$, where Φ is the applied voltage), while the experimental results exhibited rectification because of asymmetric couplings and asymmetric spatial profiles.[8]

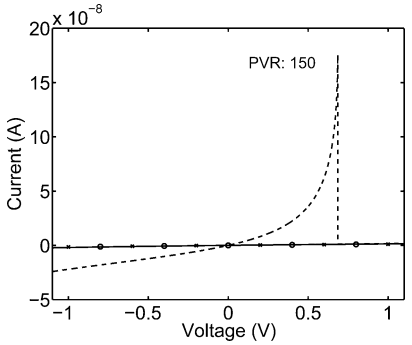

Figure 7. Asymmetric current−voltage characteristics for the molecules in Figure 1: **A** (○), **B** (x), **C** (---), and **D** (—). The values for ϵ_0 and $\tilde{\epsilon}_{\text{reorg}}$ were taken from Table 2, and the following parameters were used: $\Gamma_L = 0.04$ eV, $\Gamma_R = 0.01$ eV, and $T = 60$ K.

We therefore carried out identical calculations but with asymmetric molecule−lead couplings ($\Gamma_L = 4\Gamma_R$). The results are shown in Figure 7. For this particular asymmetric coupling, NDR is seen only for **C** and only at positive voltage (the peak is shifted to lower voltage as a result of the larger Γ_L value). Additionally, **C** exhibits mild rectification, and no NDR is seen at negative voltage as saturation is reached prior to the onset of negative bias NDR. Our calculations thus predict qualitatively different current−voltage responses for strongly asymmetric molecule−lead couplings for the two nitro compounds.

In this work, we have neglected any complexities regarding the differences in transport in SAM junctions as opposed to true single molecular devices. As the vast majority of the NDR literature with OPE molecules has consisted of SAM devices, it is still unclear as to whether[19] or not[103−105] NDR can be observed in single molecule nitro OPE systems. Future work will elaborate on the intramolecular basis of both NDR and switching behavior in general.

(102) We keep the molecule perpendicular to the surface, as there is some debate as to the packing of the OPE SAMs on gold surfaces. See refs 36 and 37. Tilting the molecule on the gold surface will of course increase the magnitude of the image charge effect.

(103) Selzer, Y.; Cabassi, M. A.; Mayer, T. S.; Allara, D. L. *Nanotechnology* **2004**, *15*, S483−S488.
(104) Selzer, Y.; Cabassi, M. A.; Mayer, T. S.; Allara, D. L. *J. Am. Chem. Soc.* **2004**, *126*, 4052−4053.
(105) Selzer, Y.; Cai, L.; Cabassi, M. A.; Yao, Y.; Tour, J. M.; Mayer, T. S.; Allara, D. L. *Nano Lett.* **2005**, *5*, 61−65.

In conclusion, we have provided a simple formalism as well as a computational method for predicting NDR behavior in molecular junctions where charging and conformational change are explained with a polaron model. This formalism also predicts hysteresis, and our future work will involve elaborating this model to explain the experimentally observed[9] temperature and voltage sweep rate dependence of hysteresis behavior. A more elaborate nonequilibrium description of the phonon degrees of freedom will be necessary, but this formal extension is necessary for a complete understanding of the memory device capabilities of molecules in junctions.

The proposed polaron model is one of many proposed explanations for NDR and switching behavior and is not a complete description of the processes in molecular devices that exhibit these characteristics. Indeed, better agreement between experimental results is necessary for further clarification of the mechanism responsible in these systems.[106] In a different experimental system (bipyridyl-dinitro oligophenylene-ethynylene dithiol), switching behavior has been seen by several groups,[107,108] and charging[109] and polaron formation[108] have been suggested as possible sources for the bistability. However, recent measurements[110] with a gate electrode have shown rare switching dependence on the gate voltage, suggesting that a charging or polaron model may not be appropriate in these systems. Calculations on these systems with the polaron model will attempt to explain the hysteresis and gate voltage dependency.[111]

Acknowledgment. We are grateful to Avik Ghosh and Smitha Vasudevan for providing us with their version of the Huckel $I-V$ 3.0 code. We also thank Abraham Nitzan, Chad Risko, Magnus Paulsson, Swapan Pati, and Jorge Seminario for helpful discussions. S.Y. acknowledges support from the Office of Naval Research through a NDSEG fellowship. Funding for this research was provided by the NSF (Network for Computational Nanotechnology, Office of International Science and Engineering, and Materials Research Science and Engineering Center at Northwestern), NASA-URETI, and DARPA-MoleApps.

Supporting Information Available: Complete ref 88; chemical structures, molecular energies. This material is available free of charge via the Internet at http://pubs.acs.org.

JA0730967

(106) Lindsay, S. M. *Faraday Discuss.* **2006**, *131*, 403−409.
(107) Blum, A. S.; Kushmerick, J. G.; Long, D. P.; Patterson, C. H.; Yang, J. C.; Henderson, J. C.; Yao, Y. X.; Tour, J. M.; Shashidhar, R.; Ratna, B. R. *Nat. Mater.* **2005**, *4*, 167−172.
(108) Lortscher, E.; Ciszek, J. W.; Tour, J.; Riel, H. *Small* **2006**, *2*, 973−977.
(109) He, J.; Fu, Q.; Lindsay, S.; Ciszek, J. W.; Tour, J. M. *J. Am. Chem. Soc.* **2006**, *128*, 14828−14835.
(110) Keane, Z. K.; Ciszek, J. W.; Tour, J. M.; Natelson, D. *Nano Lett.* **2006**, *6*, 1518−1521.
(111) Yeganeh, S.; Ratner, M. A. Unpublished work.
(112) He, J. L.; Chen, B.; Flatt, A. K.; Stephenson, J. J.; Doyle, C. D.; Tour, J. M. *Nat. Mater.* **2006**, *5*, 63−68.
(113) Amlani, I.; Rawlett, A. M.; Nagahara, L. A.; Tsui, R. K. *Appl. Phys. Lett.* **2002**, *80*, 2761−2763.
(114) Reed, M. A.; Chen, J.; Rawlett, A. M.; Price, D. W.; Tour, J. M. *Appl. Phys. Lett.* **2001**, *78*, 3735−3737.
(115) Kratochvilova, I.; Kocirik, M.; Zambova, A.; Mbindyo, J.; Mallouk, T. E.; Mayer, T. S. *J. Mater. Chem.* **2002**, *12*, 2927−2930.
(116) Li, C.; Zhang, D.; Liu, X.; Han, S.; Tang, T.; Zhou, C.; Fan, W.; Koehne, J.; Han, J.; Meyyappan, M.; Rawlett, A. M.; Price, D. W.; Tour, J. M. *Appl. Phys. Lett.* **2003**, *82*, 645−647.